

# *Ab Initio* Calculations of Light Nuclei

BRUCE R. BARRETT

*Department of Physics, University of Arizona, Tucson, Arizona, USA*

BOGDAN MIHAILA, STEVEN C. PIEPER, AND ROBERT B. WIRINGA

*Physics Division, Argonne National Laboratory, Argonne, Illinois, USA*

## Introduction

A major goal in nuclear physics is to understand how nuclear binding, stability, and structure arise from the underlying interactions between individual nucleons. We want to compute the properties of an  $A$ -nucleon system as an  $A$ -body problem with free-space interactions that describe nucleon-nucleon ( $NN$ ) scattering. Reliable *ab initio* results from such a nucleon-based model will provide a baseline against which to gauge effects of quark and other degrees of freedom. This approach will also allow the accurate calculation of nuclear matrix elements needed for some tests of the standard model, and of nuclei and processes not presently accessible in the laboratory. This can be useful for astrophysical studies and for comparisons to future radioactive beam experiments. To achieve this goal, we must both determine the Hamiltonians to be used and devise reliable methods for many-body calculations using them. Presently, we have to rely on phenomenological models for the nuclear interaction, because a quantitative understanding of the nuclear force based on quantum chromodynamics is still far in the future.

In order to make statements about the correctness of a given phenomenological Hamiltonian, one must be able to make calculations whose results reflect the properties of the Hamiltonian and are not obscured by approximations. Because the Hamiltonian is still unknown, the correctness of the calculations cannot be determined from comparison with experiment. For this reason it is essential to have a number of different *ab initio* methods which can be compared. In addition, each method should have internal consistency and convergence checks that indicate the precision of the computed results. In the last decade there has been much progress in three approaches to the nuclear many-body problem for light nuclei: no-core shell model (NCSM), Green's function Monte Carlo (GFMC), and coupled cluster expansion (CCE).

## Modern Nuclear Hamiltonians

A huge amount of  $NN$  scattering data has been collected over the last half century and has been used in the last decade to make a number of very accurate  $NN$  potentials [1]. These include the Nijm I, Nijm II, and Reid93 models of the Nijmegen group, Argonne  $v_{18}$  (AV18), and CD Bonn, which fit the  $E_{\text{lab}} \leq 350$  MeV elastic data with a  $\chi^2/\text{datum} \sim 1$ . Such modern potentials are complicated, including spin, isospin, tensor, spin-orbit, quadratic momentum-dependent, and charge-independence-breaking terms. The AV8' is a frequently used simplification of the AV18 that retains terms through the spin-orbit. Next-generation models based on chiral effective field theory, such as the Idaho models, promise a closer connection to the underlying QCD. Despite their sophistication, no modern  $NN$  model is able to reproduce the binding energies of few-body nuclei such as  ${}^3\text{H}$  and  ${}^4\text{He}$  without the assistance of a three-nucleon ( $3N$ ) potential [1].

Multi-nucleon interactions arise because of the composite nature of the nucleon and its corresponding excitation spectrum, particularly the strong  $\Delta(1232)$  resonance seen in  $\pi N$  scattering. Due to the large cancellation between one-body kinetic and two-body potential energies, they can provide significant corrections to nuclear binding. Fortunately,  $4N$  potentials appear small enough to be ignored at present. Models for the basic two-pion-exchange  $3N$  potential date from the 1950s. More sophisticated models have followed, including the Tucson-Melbourne model with partially conserved axial current constraints, a chirally-improved version, TM', the Urbana series which incorporate short-range repulsion, and the Illinois models which add multi-pion rings [1, 2].

In principle, the  $3N$  potential could have a far more complicated dependence on the spins, isospins, and momenta of the nucleons than has been studied to date, but there is limited information by which to constrain the

models. Three-nucleon scattering data can help for total isospin  $T = 1/2$  systems, but are not available for  $T = 3/2$  systems. The binding energies and excitation spectra of light nuclei provide the best constraints for  $3N$  potentials, especially for  $T = 3/2$  interactions, which are particularly important for neutron stars.

### Ab Initio methods

#### No Core Shell Model

The NCSM is based on a new variation of the well-known shell model for nuclei. Historically shell-model calculations have been made assuming a closed, inert core of nucleons with only a few active valence nucleons. The interaction of these valence nucleons with the core and with other valence nucleons could not be described by microscopic interactions, as they have been developed for few-nucleon systems. Therefore, these attempts have not been completely successful in relating the effective shell-model interaction to the basic nuclear interaction.

This situation changed in 1990 with the development of the NCSM, which treats all nucleons in the nucleus as active particles. One starts with the relative (or translationally invariant) Hamiltonian for all  $A$  nucleons and adds the harmonic-oscillator (HO) center-of-mass (CM) potential. This provides a confining potential, necessary for the computation of the effective interaction, as well as a basis, i.e., the HO basis, for performing detailed calculations. The effects of the CM interaction can be easily separated and later subtracted. The strong correlations of nucleons in nuclei, however, lead to slowly converging results in the HO basis. Therefore, shell-model calculations based on “bare” interactions are generally not useful. The solution of this dilemma is the utilization of “effective” interactions. Because the NCSM assumes that all nucleons are active, there is a systematic way to obtain the effective interactions from bare  $NN$  and  $3N$  forces [3, 4]. This is the strength of the NCSM compared to traditional shell-model calculations.

If the infinite HO basis space is divided into a model space and an excluded space by the use of projection operators  $P$  and  $Q$ , respectively, the effective Hamiltonian  $H_{\text{eff}}$  is obtained by performing a similarity transformation,  $X$ , on the original Hamiltonian,  $H$ , and imposing the decoupling condition  $QXH X^{-1}P = 0$ ; i.e.,  $H_{\text{eff}}$  has no matrix elements between the  $P$  and  $Q$  spaces. Unfortunately, the exact determination of  $X$  requires the solution of the full  $A$ -body problem; however, the determination of  $H_{\text{eff}}$ , based on the solution of the two- or three-body cluster problem, results in an excellent approximation.

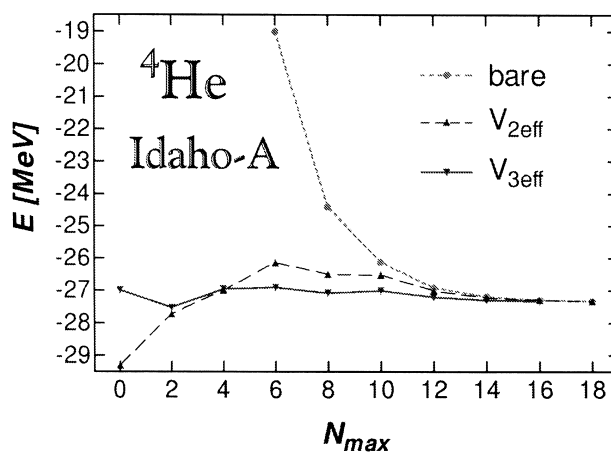


Figure 1. NCSM convergence for  ${}^4\text{He}$  for bare and effective interactions.

Thereby, it is ensured that one recovers the bare problem, if the model space approaches the full space, so that the approximation is fully controllable. The method for obtaining the two-body effective interaction in the  $P$  space is completely general [4] and can be applied to any current modern  $NN$  potential in either coordinate or momentum space.

The effective two-body interactions determined from these modern  $NN$  potentials were first applied to no-core calculations for  ${}^3\text{H}$  and  ${}^4\text{He}$ , where traditional shell-model calculations are slowly converging, but where few-body techniques are applicable. The NCSM results for these nuclei are in line with several other methods [5].

Figure 1 shows the results for  ${}^4\text{He}$  as a function of the size of the model space  $P$  in terms of  $N_{\text{max}} - \Omega$ , the maximum HO energy above the unperturbed ground-state configuration. The figure also demonstrates that the convergence is accelerated tremendously by the use of the effective interactions. We show results for both two- and three-body effective interactions [3]. Because the three-body effective interactions can take higher-order correlations into account, they can improve the convergence even more than the two-body ones, as seen in Figure 1, especially for small  $N$ . Three-body effective interactions are unavoidable, if one wants to employ bare three-body interactions. Work on this issue is in progress. In summary, from three- and four-body nuclei, one learns that the utilization of the effective NCSM interaction is a useful and feasible way to improve conver-

gence for shell-model calculations and, at the same time, maintain the connection to microscopic nuclear interactions. Based on this knowledge, the method has been applied to nuclei in the  $A \leq 16$  mass region.

To this aim, the  $NN$  or  $3N$  problem with confining HO interaction is solved [3, 4] and the solutions are used to obtain effective interactions for the  $A$ -body problem. The model space is restricted by the maximal excitation  $N_{max}$ . Reasonably converged calculations for, e.g.,  $^{12}\text{C}$ , have been obtained with  $N_{max} = 6$  [4]. Using standard Lanczos iteration algorithms, not only the ground, but also excited states are obtained and, consequently, the low-lying spectrum can be investigated. At the same time one gets the nuclear wave functions corresponding to the effective nuclear Hamiltonian. First steps to calculate matrix elements based on the corresponding effective operators have been done, but more work in this direction is still necessary in the future.

Much effort in the recent past has been devoted to the development of parallelizable procedures to handle the computations on massively parallel computers. This is a highly nontrivial task, because of the extensive book-keeping involved. Efficient integer arithmetic and fast communication are necessary to achieve high performance. Future developments in both the computer hardware and our algorithms will enable us to obtain the spectra for the whole range of  $p$ -shell nuclei based on  $NN$  and  $3N$  forces and may allow investigations of some  $sd$ -shell nuclei.

### *Green's Function Monte Carlo*

The first application of Monte Carlo methods to nuclei interacting with realistic potentials was a variational (VMC) calculation by Pandharipande and collaborators [6], who computed upper bounds to the binding energies of  $^3\text{H}$  and  $^4\text{He}$  in 1981. Six years later, Carlson [7] improved on the VMC results by using the Green's function Monte Carlo (GFMC) algorithm, obtaining essentially exact results (within Monte Carlo statistical errors of 1%). Reliable calculations of light  $p$ -shell nuclei started to become available in the mid-1990s and are reviewed in [2]; the most recent results for  $A = 10$  nuclei can be found in [8].

A VMC calculation finds an upper bound,  $E_T$ , to an eigenvalue of the Hamiltonian,  $H$ , by evaluating the expectation value of  $H$  using a trial wave function,  $\Psi_T$ . The parameters in  $\Psi_T$  are varied to minimize  $E_T$ , and the lowest value is taken as the approximate energy. Over the years, rather sophisticated  $\Psi_T$  for light nuclei have been developed [2]. These contain symmetrized products

over all pairs of (non-commuting) two-body operators (the most important being the tensor-isospin correlation corresponding to the pion-exchange potential) and sums of non-central three-body correlations induced by the  $3N$  interaction. These act on a Jastrow wave function which contains a product over all pairs of a central pair correlation and an antisymmetric one-body piece. The main effect of the central pair correlation is to keep nucleons from getting too close to the strong short-range repulsive core of the  $NN$  potential. The one-body piece determines the quantum numbers and antisymmetry of the state being computed; the wave function is translationally invariant.

The  $\Psi_T$  is a vector in the spin-isospin space of the  $A$  nucleons, each component of which is a complex-valued function of the positions of all  $A$  nucleons. The tensor correlations mix spin and spatial angular momenta, so that all  $2^A$  spin combinations appear. The conservation of isospin results in fewer isospin possibilities, somewhat less than  $\binom{A}{2}$ . The total numbers of components in the vectors are 16, 160, 1792, 21 504, and 267 168 for  $^4\text{He}$ ,  $^6\text{Li}$ ,  $^8\text{Be}$ ,  $^{10}\text{B}$ , and  $^{12}\text{C}$ , respectively.

GFMC [2] projects out the lowest-energy eigenstate from the VMC  $\Psi_T$  by using

$$\Psi_0 = \lim_{\tau \rightarrow \infty} \Psi(\tau) = \lim_{\tau \rightarrow \infty} \exp[-(H - E_0)\tau] \Psi_T.$$

If sufficiently large  $\tau$  is reached, the eigenvalue  $E_0$  is calculated exactly while other expectation values are generally calculated neglecting terms of order  $|\Psi_0 - \Psi_T|^2$  and higher. In contrast, the error in the variational energy,  $E_T$ , is of order  $|\Psi_0 - \Psi_T|^2$ , and other expectation have errors of order  $|\Psi_0 - \Psi_T|$ .

The evaluation of  $\exp[-(H - E_0)\tau]$  is made by introducing a small time step,  $\Delta\tau = \tau/n$  (typically  $\Delta\tau = 0.5 \text{ GeV}^{-1}$ ),

$$\Psi(\tau) = \{\exp[-(H - E_0) \Delta\tau]\}^n \Psi_T = G^n \Psi_T;$$

where  $G$  is the short-time Green's function. In coordinate space this results in a multidimensional integral over  $3An$  (typically more than 10,000) dimensions which is done by Monte Carlo. The short-time propagator is approximated as a symmetrized product of exact two-body propagators and includes the  $3N$  potential to first-order. The errors introduced by these approximations can be made arbitrarily small by reducing  $\Delta\tau$  (and increasing  $n$ ). In recent benchmark calculations [5] of  $^4\text{He}$  using the AV8' potential, the GFMC energy had a statistical error of only 20 keV and agreed with the other

best results to this accuracy (<0.1%). Various tests indicate that the GFMC calculations of  $p$ -shell binding energies have errors of 1–2%.

For more than four nucleons, GFMC calculations suffer significantly from the well-known fermion sign problem. This results in exponential growth of the statistical errors as one propagates to larger  $\tau$ , or as  $A$  is increased. For  $A \geq 8$  the resulting limit on  $\tau$  is too small to allow convergence of the energy. This problem is solved by using a constrained-path algorithm, in which configurations with small or negative  $\Psi(\tau)^\dagger \cdot \Psi_T$  are discarded such that the average over all discarded configurations of  $\Psi(\tau)^\dagger \cdot \Psi_T$  is zero. Thus, if  $\Psi_T$  were the true eigenstate, the discarded configurations would contribute nothing but noise to  $\langle H \rangle$ . To eliminate possible bias, a final few (10–20) unconstrained steps are made before evaluating the energy.

As described above, the number of spin-isospin components in  $\Psi_T$  grows rapidly with the number of nucleons. Thus, a calculation of a state in  ${}^8\text{Be}$  involves about 30 times more floating-point operations than one for  ${}^6\text{Li}$ , and  ${}^{10}\text{B}$  requires 25 times more than  ${}^8\text{Be}$ . Calculations of the sort being described are currently feasible up to only  $A = 10$ ; these require  $\sim 10,000$  processor hours on modern massively parallel computers, or  $\sim 10^{16}$  floating point operations, for a single state.

### Coupled Cluster Expansion

The coupled-cluster expansion (CCE), also called the exp(S) method, was developed in the early 1960s by Coester and Kümmel [9]. While the method is exact, approximations are introduced stemming from truncations in the CCE equations, as well as truncations in the model space. Practical approaches for nuclear structure applications have been notoriously difficult to realize. It was not until the 1970s that Zabolitsky and Kümmel [10] made the first detailed calculations for finite nuclei, using a representation of the wave function in coordinate space together with common interactions of the time. Further developments have proved difficult to achieve, and the method lay dormant for another 25 years. Motivated by the availability of more sophisticated NN interactions, and riding the wave of the ongoing expansion in computer power, Heisenberg and Mikhaila [11] reexamined the CCE and applied it to the spherical nucleus  ${}^{16}\text{O}$ .

The CCE formalism relies on expanding the nuclear wave function in terms of two abelian subalgebras of multi-configurational creation and their Hermitian-

adjoint destruction operators, where the expansion coefficients represent the nuclear correlations. Presently, the CCE equations are solved in configuration space.

One considers first the case of the ground-state  $|\Psi\rangle$ , of a spin-isospin shell-saturated nucleus, such as  ${}^4\text{He}$ ,  ${}^{12,14}\text{C}$ ,  ${}^{14,16}\text{O}$ . We have  $|\Psi\rangle = e^{\tilde{S}}|\Phi\rangle$ . Here  $|\Phi\rangle$  represents the physical vacuum, defined such that  $\mathbf{a}_b^\dagger|\Phi\rangle = \mathbf{a}_p|\Phi\rangle = 0$ . The cluster correlation operator is introduced in terms of its  $ph$ -creation operator expansion,  $S^\dagger = \sum 1/n! S_n \mathbf{O}_n^\dagger$ , with  $\mathbf{O}_n^\dagger = \{1, \mathbf{a}_{p_1}^\dagger \mathbf{a}_{b_1}, \mathbf{a}_{p_2}^\dagger \mathbf{a}_{p_1}^\dagger \mathbf{a}_{b_1} \mathbf{a}_{b_2}, \dots\}$ . The ground-state energy,  $E$ , and the amplitudes  $S_n$ , are obtained by solving a set of formally exact coupled nonlinear equations

$$E = \langle \Phi | e^S H e^{-S} | \Phi \rangle,$$

$$0 = \langle \Phi | e^S H e^{-S} \mathbf{O}_n^\dagger | \Phi \rangle, n \leq A.$$

The procedure involves obtaining the G-matrix interaction together with a self-consistent calculation of the mean-field spectrum of single-particle energies and wave functions. Truncations of the above set of equations involve decisions regarding contributions to the  $2p2h$ ,  $3p3h$ ,  $4p4h$ ,  $\dots$  sectors. The present code treats the  $2p2h$ -sector completely;  $3p3h$  and  $4p4h$  correlations are included by means of a series expansion in powers of  $S_2$ .

The expectation value of an arbitrary operator  $\hat{O}$ , is defined as  $\langle \hat{O} \rangle = \langle \Phi | e^S \hat{O} e^{-S} \tilde{S}^\dagger | \Phi \rangle$ , where  $\tilde{S}^\dagger$  is also defined by a decomposition in terms of  $ph$ -creation operators,  $\tilde{S}^\dagger = \sum 1/n! \tilde{S}_n \mathbf{O}_n^\dagger$ . The amplitudes  $\tilde{S}_n$  are obtained in terms of  $S_n$  in an iterative fashion. Note that the correlated ground-state  $|\Psi\rangle$  is not translationally invariant: a many-body expansion has been devised to calculate observables in the CM frame [12].

The excited-state spectrum of the spherical nucleus, and the spectrum of neighboring nuclei, such as  ${}^{13}\text{C}$  and  ${}^{15}\text{N}$ , are subsequently described relying on the ground state of the spherical nucleus as a *new* vacuum. One defines complete sets of many-body excitation modes,  $\mathbf{B}_n^\dagger$ , which are orthogonal to  $|\Psi\rangle$ . These modes are given in terms of complete sets of operators  $\mathbf{C}_n$ , such that  $\mathbf{B}_n = e^{\tilde{S}} \mathbf{C}_n e^{-\tilde{S}}$  satisfy  $\mathbf{B}_n |\Psi\rangle = \mathbf{C}_n |\Phi\rangle = 0$ . For illustrative purposes, let us consider the case of a hole-state nucleus, such as  ${}^{15}\text{N}$ . Begin by defining  $\mathbf{C}_n^\dagger = \{\mathbf{a}_{b_1}, \mathbf{a}_{p_1}^\dagger \mathbf{a}_{b_1} \mathbf{a}_{b_2}, \dots\}$  and write an arbitrary state  $|\Psi_j\rangle$  of  ${}^{15}\text{N}$  as a linear combination of the many-body excitation modes above:  $|\Psi_j\rangle = \Omega_j^\dagger |\Psi\rangle = \sum X_{n(j)} \mathbf{B}_n |\Psi\rangle$ . The expansion coefficients  $X_{n(j)}$ , and the excitation energies  $E_j$ , are obtained by solving the equation of motion

$$E_j \Omega_j^\dagger |\Psi\rangle = [\mathbf{H}, \Omega_j^\dagger] |\Psi\rangle.$$

Table 1. Comparison of GFMC and NCSM energies in MeV.

|                        | GFMC     | NCSM   | Difference |
|------------------------|----------|--------|------------|
| ${}^8\text{Be}(0^+)$   | -47.9(1) | -48.5  | -0.6       |
| ${}^8\text{Be}(2^+)$   | -45.6(1) | -44.8  | 0.8        |
| ${}^8\text{Be}(4^+)$   | -38.7(1) | -36.1  | 1.6        |
| ${}^8\text{Be}(1^+)$   | -32.8(1) | -31.1  | 1.6        |
| ${}^8\text{Be}(3^+)$   | -31.2(1) | -29.6  | 1.7        |
| ${}^{10}\text{B}(1^+)$ | -55.7(3) | -56.19 | -0.5       |
| ${}^{10}\text{B}(3^+)$ | -53.2(3) | -54.83 | -1.6       |
| ${}^{10}\text{B}(2^+)$ | -52.2(2) | -53.36 | -1.2       |
| ${}^{10}\text{B}(4^+)$ | -50.0(4) | -50.10 | -0.1       |

The limitations of the configuration-space approach to solving the CCE equations derive from the intrinsic cutoffs imposed on the model space. In effect one presently discretizes the continuum part of the one-body mean-field Hamiltonian used to define the single-particle spectrum. This results in a large,  $50 \text{ } \Omega$ , configuration space, and consequently significant storage and lengthy execution time. These requirements ( $\sim 1.5$  GB disk space, and 1 week CPU time for the ground state of  ${}^{16}\text{O}$ ), are modest compared to the GFMC computational needs.

## Results

Because of space limitations, we can present only a few of the results that have been obtained with the three methods. Additional calculations of energies and other nuclear properties can be found in the references. Table 1 shows a comparison of GFMC and NCSM results for the AV8' NN potential for the examples of  ${}^8\text{Be}$  and  ${}^{10}\text{B}$ . GFMC statistical errors are shown in parentheses; as discussed above there are also systematic errors. The binding energies are mostly in agreement within the expected errors, which is very encouraging. The very broad  ${}^8\text{Be}(4^+)$  level, which should be treated as a scattering state, is an exception.

Another comparison, which also shows the importance of effective operators in NCSM calculations, is provided by the NN pair density computed for  ${}^4\text{He}$  with AV8' (Figure 2). The NCSM result obtained with the effective operator is in good agreement with the GFMC result, but the density based on the "bare" operator is wrong. This shows that one must use effective operators, which are well-defined, in NCSM matrix element calculations. The figure also shows that in the NCSM calculations the short-range repulsion in the NN system is not represented in the wave function, but in the operators.

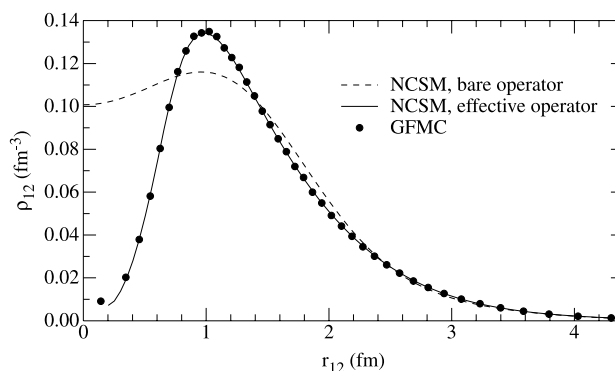


Figure 2. NCSM and GFMC NN pair density in  ${}^4\text{He}$ .

This is the key to the improved convergence obtained by the use of effective interactions.

Figure 3 compares GFMC calculations of energy levels of some selected  $p$ -shell nuclei with the experimental values. The calculations use just the AV18 NN potential (left bars) and the AV18 with the Illinois-2 (IL2) 3N potential [2]. The figure shows that calculations with just NN potentials significantly underbind the nuclei, with the underbinding getting worse as  $A$  increases. In addition, many spin-orbit splittings, such as that of the  $(5-/2) - (7-/2)$  levels in  ${}^7\text{Li}$ , are too small. The IL2 corrects these errors and results in good agreement with the data; for 53 levels in  $3 \leq A \leq 10$  nuclei the rms deviation from experiment is only 740 keV. The case of  ${}^{10}\text{B}$  is particularly interesting. The calculation with just AV18 incorrectly produces a  $1^+$  ground state instead of the observed  $3^+$ . NCSM calculations get the same result using CD-Bonn, so this is a general failure of Hamiltonians

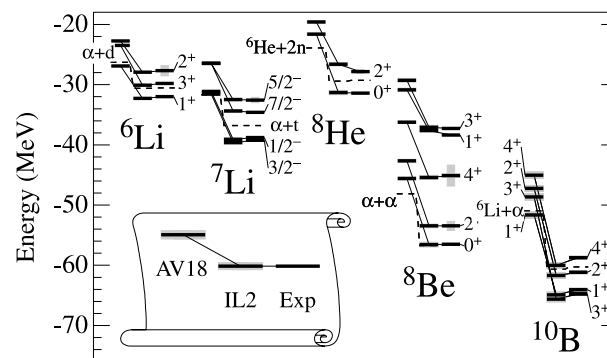


Figure 3. GFMC energies without and with a 3N force.

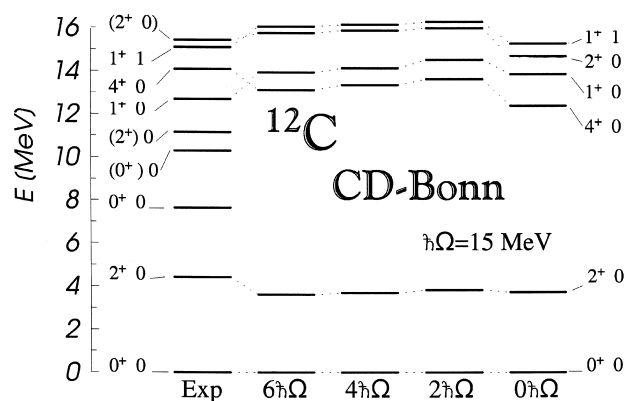


Figure 4. Experimental and NCSM excitation spectra for  $^{12}\text{C}$  for different model space sizes.

based on  $NN$  potentials only. As the figure shows, including IL2 reverses the order of the two levels and produces the correct ground state. In fact, as discussed by Kurath in 1956 [13], this can be understood as another manifestation of  $3N$  potentials correcting the spin-orbit splitting.

Figure 4 shows the low-lying spectrum of  $^{12}\text{C}$  for different NCSM model-space sizes, compared with experiment. Clearly, the first-excited states show an indication of convergence. The calculated results agree very well with experiment for the first  $2^+$  state. The second and third  $0^+$  and the second  $2^+$  states cannot be reproduced by the calculations, probably because they are dominated by  $N = 2$  excitations and are, therefore, intruder states. Interestingly, the calculation using only the  $NN$  force predicts the wrong level ordering of the  $4^+$  and  $1^+$  states. The first  $1^+$  and  $4^+$  levels are influenced by spin-orbit strength [13] and so including  $3N$  potentials will be of special interest for future investigations.

In Figure 5 we compare a CCE calculation [11] of the  $^{16}\text{O}$  charge form factor, using AV18 supplemented by the Urbana IX  $3N$  interaction, with electron scattering data [14]. The calculation includes meson-exchange currents, and accounts for the distortions due to the interaction of the electron with the Coulomb field. The calculated value for the binding energy of  $^{16}\text{O}$  is 7.54 MeV/nucleon, to be compared with the experimental value of 8 MeV/nucleon. The form factor is in good agreement with experiment, and the energy is reasonable for this Hamiltonian.

An important aspect of light  $p$ -shell nuclei is the tendency of the nucleons to cluster into tritons, alphas, etc., as evidenced by the breakup thresholds shown in Figure

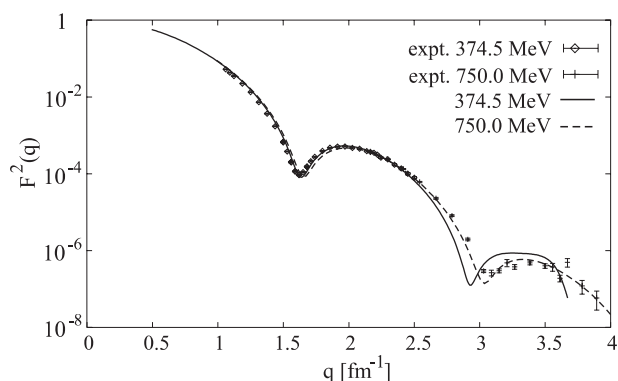


Figure 5. CCE charge form factor for  $^{16}\text{O}$ .

3. This feature is not readily apparent in the one-body part of the GFMC  $\Psi_T$ , which consists of an alpha core and  $A-4$   $p$ -shell nucleons. However, the pair correlations in  $\Psi_T$  provide significant clustering, as is shown in Figure 6, which gives GFMC density contours for  $^8\text{Be}(0^+)$  in cylindrical coordinates. The left portion of the figure shows the laboratory frame density, which is spherically symmetric. The right portion shows the body-fixed density. Two regions of high density are clearly evident, which are identified as two alpha particles. The corresponding figures for the  $2^+$  and  $4^+$  states are quite different in the laboratory frame, but all three are the same in the body-fixed frame. Thus the  $\Psi_T$  used in GFMC calculations quite naturally includes few-nucleon clustering.

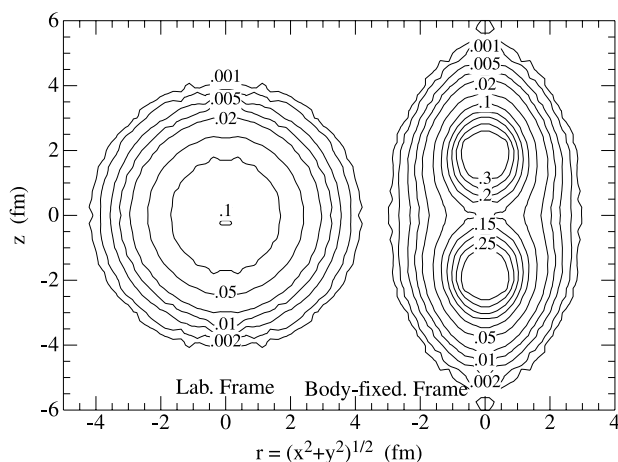


Figure 6. GFMC density contours for  $^8\text{B}(0^+)$ .

## Conclusions

The results of these *ab initio* methods are highly encouraging, because they indicate that it is now possible to perform accurate calculations of nuclear properties, such as binding energies and pair densities, for which the different methods agree. This opens the way to applying these methods to calculations of other physical observables. The ability to reliably predict binding energies based on realistic Hamiltonians also enables further research to determine the  $3N$  force.

Besides the study of specific properties of  $p$ -shell nuclei, such as super-allowed Fermi beta decay for  $A = 10$  or the Gamow Teller strength for  $A = 14$ , there are particular goals of the different methods. Within the NCSM approach, the inclusion of four-body effective forces will allow better tests of the convergence with increasing cluster level. But the most exciting next project will be a study of the effects of different  $3N$  forces on the spectra.

The VMC trial functions that serve as a starting point for GFMC calculations have been used in a number of applications, including studies of electromagnetic elastic and transition form factors in  ${}^6\text{Li}$ , spectroscopic factors in the  ${}^7\text{Li}(e, e'p)$  reaction, transition densities for pion scattering in  ${}^6\text{Li}$  and  ${}^7\text{Li}$ , and weak decay rates for  ${}^6\text{He}$  and  ${}^7\text{Be}$  [2]. They have also been used to study astrophysically interesting radiative capture reactions such as  $t(\alpha, \gamma){}^7\text{Li}$  and  ${}^3\text{He}(\alpha, \gamma){}^7\text{Be}$  [15]. These calculations use microscopic one- and two-body operators; no effective charges are required. The results are generally in good agreement with experiment, but it is important to repeat these calculations with the more accurate GFMC wave functions. Many additional electroweak matrix elements remain to be calculated, particularly in  $A \geq 8$  nuclei. An important challenge for the future is to treat resonant states as actual scattering states and not as pseudo-bound states.

The methods described here have distinctly different possible growth paths. The GFMC will probably be extended to  ${}^{12}\text{C}$  in the next few years, but it will not be feasible beyond that because of the exponential growth of the spin-isospin vector size. However, the auxiliary field diffusion Monte Carlo [16], which is closely related, has been used for much larger pure neutron systems and is currently being studied for nuclei. The NCSM should be capable of being extended to light  $sd$ -shell nuclei. In ad-

dition, the knowledge of two- and three-body effective interactions being developed for the NCSM could find use in other types of shell model calculations for heavier nuclei. Finally, the CCE can potentially be used for much larger nuclei; in the 1970s it was already applied to  ${}^{40}\text{Ca}$  by Zabolitzky [10].

## Acknowledgments

The work described here was done by many more researchers than just the authors, notably P. Navrátil, A. Nogga, W. E. Ormand, and J. P. Vary for the NCSM; J. Carlson, V. R. Pandharipande, and B. S. Pudliner for the GFMC; and J. Heisenberg for the CCE. The work of BRB is supported in part by NSF grant No. PHY0070858, and that of BM, SCP, and RBW by the U.S. Department of Energy, Nuclear Physics Division, under contract W-31-109-ENG-38.

## References

1. J. Carlson and R. Schiavilla, *Rev. Mod. Phys.* **70**, 743 (1998), and references therein.
2. S. C. Pieper and R. B. Wiringa, *Annu. Rev. Nucl. Part. Sci.* **51**, 53 (2001), and references therein.
3. P. Navrátil and W. E. Ormand, *Phys. Rev. Lett.* **88**, 152502 (1002), and references therein.
4. P. Navrátil, J. P. Vary, and B. R. Barrett, *Phys. Rev. Lett.* **84**, 5728 (2000); *Phys. Rev. C* **62**, 054311 (2000), and references therein.
5. H. Kamada et al., *Phys. Rev. C* **64**, 044001 (2001).
6. J. Lomnitz-Adler, V. R. Pandharipande, and R. A. Smith, *Nucl. Phys.* **A361**, 399 (1981)
7. J. Carlson, *Phys. Rev. C* **36**, 2026 (1987).
8. S. C. Pieper, K. Varga, and R. B. Wiringa. *Phys. Rev. C* **66**, 034611 (2002).
9. F. Coester, *Nucl. Phys.* **7**, 421 (1958); F. Coester and H. Kümmel, *Nucl. Phys.* **17**, 477 (1960).
10. H. Kümmel, K. H. Lührmann, and J. G. Zabolitzky, *Phys. Reports* **36**, 1 (1978).
11. B. Mihaila and J. H. Heisenberg, *Phys. Rev. C* **61**, 054309 (2000), and references therein.
12. B. Mihaila and J. H. Heisenberg, *Phys. Rev. C* **60**, 054303 (1999).
13. D. Kurath, *Phys. Rev.* **101**, 216 (1956).
14. I. Sick and J. S. McCarthy, *Nucl. Phys. A* **150**, 631 (1970).
15. K. M. Nollett, *Phys. Rev. C* **63**, 054002 (2001).
16. S. Fantoni, A. Sarsa, and K. E. Schmidt, *Phys. Rev. Lett.* **87**, 181101 (2001).